

1

An overview

1.1 The Cahn-Hilliard equation

We shall focus in this text on the Cahn-Hilliard equation:

$$u_t = \nabla \cdot M(u) \nabla [f(u) - \epsilon^2 \Delta u], \quad (x, t) \in \Omega \times R^+, \quad (1.1)$$

$$n \cdot \nabla u = n \cdot M(u) \nabla [f(u) - \epsilon^2 \Delta u] = 0, \quad (x, t) \in \partial\Omega \times R^+, \quad (1.2)$$

$$u(x, 0) = u_0(x), \quad x \in \Omega, \quad (1.3)$$

where $0 < \epsilon^2 \ll 1$ is a "coefficient of gradient energy," $M = M(u)$ is a mobility coefficient, and $f = f(u)$ is a "homogeneous free energy." Here $u = u(x, t)$, whose evolution is prescribed by the Cahn-Hilliard equation given above, represents the *concentration* of one of the components of a two component system occupying the "volume" Ω and n is a unit exterior normal to Ω . Throughout the majority of our discussions, the domain of definition of the problem, Ω , will be assumed to be a bounded domain which possesses a "sufficiently smooth" boundary $\partial\Omega$. We shall be more specific about the required regularity in the sequel. Evolution will always be considered either for all times $t > 0$ as in the formulation given in (1.1)-(1.3) or on some finite interval $0 < t < T < \infty$.

Concentration should be understood as representing either *volume fraction* or *mass fraction*, depending on the physical system under investigation. For example, if $u(x, t)$ is to be interpreted as *volume fraction* in a system containing two components which we shall denote by "A" and "B," then $u(x, t) = V_A/V$, where V_A (V_B) represents the volume of component "A" ("B") in a given arbitrarily small volume $V = V_A + V_B$ containing the point x . Clearly this corresponds to a continuous as opposed to a discrete or lattice description of the material which is appropriate under many but not all circumstances. Note in particular that

this definition implies that $u(x, t)$ should satisfy $0 \leq u(x, t) \leq 1$. Moreover, we see that if $u(x, t)$, the concentration of component A , is known, then the concentration of the second component is given by $1 - u$ and is hence also known. This allows us to ascertain the composition of the material via the solution of a single evolution equation.

In the context of the Cahn-Hilliard equation, the two component system could refer, for example, to a two component metallic system, such as iron and aluminum, or a two component polymer system. We remark that in materials science literature, concentration is given most often not in terms of volume fraction or mass fraction, but in terms of *mole fraction*. A mole refers to 6.02252×10^{23} molecules (Avogadro's number of molecules), and hence the mole fraction is equal to the number fraction, $N_A/(N_A + N_B)$, in an arbitrarily small volume V , where N_A is the number of A molecules in V and $N = N_A + N_B$ is the total number of molecules in V . Thus mole fraction and number fraction are equivalent to volume fraction if the molar volume (the volume occupied by one mole) is independent of composition; this is frequently assumed, but is rarely strictly correct [13]. The appropriateness of the Cahn-Hilliard equation often entails various approximations. Noticeably the model is isothermal, and hence is appropriate only under carefully temperature controlled circumstances. Also, for example, in two component polymer systems when the polymers are long, the polymer spatial configuration is typically compositionally dependent, which in turn influences the molar volume. The Cahn-Hilliard equation has also appeared as the modelling equation in numerous other contexts with very disparate length scales. For example, models have been developed in which the Cahn-Hilliard equation is used to represent the evolution of two components of intergalactic material or in ecology in the modeling of the dynamics of two populations or in biomathematics in modeling the dynamics of the biomass and the solvent components of a bacterial film.

Why does the Cahn-Hilliard equation appear in so many different contexts, and what behavior is predicted by the Cahn-Hilliard equation which is common to all these systems? Off-hand, what is being modelled with the Cahn-Hilliard equation is phase separation in the presence of a mass constraint, and what one wishes to accomplish here is to model the dynamics in a sufficiently accurate fashion so that many of the various features of the pattern formation evolution that one sees in nature during phase separation can be explained and predicted. In materials science this pattern formation is referred to as the *microstructure* of the material, and the microstructure is highly influential in determining

many of the properties of the material, such as strength, hardness, and conductivity. See Figure 1.1. The Cahn-Hilliard model can be seen to be rather broad ranged in its evolutionary scope in that it can serve as a good model for many systems at early times, it can give a reasonable qualitative description for these systems during intermediary times, and it can serve as a good model for even more systems at late times. Often, the late time evolution is so slow that the pattern formation or microstructure becomes effectively frozen into the system over time scales of interest, and hence it is the long time behavior of the system which is seen in practise. Our goal is to understand the predictions of the Cahn-Hilliard equation, and to see what are its successes and its drawbacks. Clearly, though, it is successful in mimicking many of the features of phase separation dynamics, and whether one should be surprised by its successes, or disappointed by its failures to describe even more, is, of course, a matter of personal taste.

We hope that by the time the reader has read through this overview, the notions of backwards diffusion and surface diffusion and their connection with the Cahn-Hilliard equation will have been clarified, and some general picture will have been conveyed of the nature of the physical phenomena which accompany phase separation and the ability of the Cahn-Hilliard equation to captured these features. A first step towards understanding the behavior encoded in the Cahn-Hilliard equation is to understand the phenomenon of backwards diffusion.

1.2 Backwards diffusion and regularization

Let us suppose that $f(u) = -u + u^3$, and that $M(u) = M_0$, where M_0 is a positive constant, and let us consider $t \in (0, T)$, $0 < T < \infty$, and $\Omega = (0, L)$. In most applications, $\Omega \in R^n$ with $n = 2$ or $n = 3$ is most physically relevant. However, for simplicity we shall focus temporarily on the bounded $n = 1$ case. Thus,

$$u_t = M_0[-u + u^3 - \epsilon^2 u_{xx}]_{xx}, \quad (x, t) \in (0, L) \times (0, T), \quad (1.4)$$

$$u_x = M_0[-u + u^3 - \epsilon^2 u_{xx}]_x = 0, \quad (x, t) \in \{0, L\} \times (0, T), \quad (1.5)$$

$$u(x, 0) = u_0(x), \quad x \in (0, L). \quad (1.6)$$

Note that $u(x, t) = \frac{1}{2}$ constitutes a steady state of (1.4)-(1.5) which corresponds to a system containing equal amounts of each component. Indeed $u(x, t) = k$ constitutes a steady state of (1.4)-(1.5), where k is

an arbitrary constant; however if $u(x, t)$ is to represent concentration, then clearly one must have that $0 \leq k \leq 1$. Let us now suppose that $u_0 = \frac{1}{2} + \tilde{u}_0$, where $\tilde{u}_0(x)$ represents a small initial perturbation from spatial uniformity. Accordingly, assuming that the problem is well posed and there is continuity from the initial data, and that $u(x, t) = \frac{1}{2} + \tilde{u}(x, t)$ is the solution for times $0 < t \ll 1$, then $\tilde{u}(x, t)$ represents a small perturbation from spatial and temporal uniformity which can be assumed to be smooth, and (1.4)-(1.6) yields that

$$\tilde{u}_t = M_0[-\tilde{u} + [\frac{1}{2} + \tilde{u}]^3 - \epsilon^2 \tilde{u}_{xx}]_{xx}, \quad (x, t) \in (0, L) \times (0, T), \quad (1.7)$$

$$\tilde{u}_x = M_0[-\tilde{u} + [\frac{1}{2} + \tilde{u}]^3 - \epsilon^2 \tilde{u}_{xx}]_x = 0, \quad (x, t) \in \{0, L\} \times (0, T), \quad (1.8)$$

$$\tilde{u}(x, 0) = \tilde{u}_0(x) := u_0(x) - \frac{1}{2}, \quad x \in (0, L). \quad (1.9)$$

Since \tilde{u} has been assumed to be small[†], we have that

$$\left[\frac{1}{2} + \tilde{u}\right]^3 \approx \frac{1}{8} + \frac{3}{4}\tilde{u} + \mathcal{O}(\tilde{u}^2).$$

Hence the equation and the boundary and initial conditions should behave roughly as

$$\tilde{u}_t = M_0 \left[-\frac{1}{4}\tilde{u} - \epsilon^2 \tilde{u}_{xx} \right]_{xx}, \quad (x, t) \in (0, L) \times (0, T), \quad (1.10)$$

$$\tilde{u}_x = M_0 \left[-\frac{1}{4}\tilde{u} - \epsilon^2 \tilde{u}_{xx} \right]_x = 0, \quad (x, t) \in \{0, L\} \times (0, T), \quad (1.11)$$

$$\tilde{u}(x, 0) = \tilde{u}_0(x), \quad x \in (0, L). \quad (1.12)$$

We recall that we have assumed earlier that $0 < \epsilon^2 \ll 1$. Suppose that we optimistically neglect terms in the system (1.10)–(1.12) which contain a factor of ϵ^2 . Since we have assumed that $M_0 > 0$, formally we obtain in this manner that

$$\tilde{u}_t = -\frac{M_0}{4}\tilde{u}_{xx}, \quad (x, t) \in (0, L) \times (0, T), \quad (1.13)$$

$$\tilde{u}_x = 0, \quad (x, t) \in \{0, L\} \times (0, T), \quad (1.14)$$

$$\tilde{u}(x, 0) = \tilde{u}_0(x), \quad x \in (0, L). \quad (1.15)$$

Let us now recall that the "regular" diffusion equation (which is equally well known as the "heat equation") with Neumann boundary conditions,

[†] We remark that while in this first chapter our analysis will be given on somewhat of a qualitative level, many if not all of the topics covered here will be revisited in later chapters with enhanced rigor, with precise reference to appropriate function spaces, etc.

can be written as

$$\tilde{u}_t = \frac{M_0}{4} \tilde{u}_{xx}, \quad (x, t) \in (0, L) \times (0, T), \quad (1.16)$$

$$\tilde{u}_x = 0, \quad (x, t) \in \{0, L\} \times (0, T), \quad (1.17)$$

$$\tilde{u}(x, 0) = \tilde{u}_0(x), \quad x \in (0, L). \quad (1.18)$$

We remark that the approximating system (1.13)–(1.15) which was obtained above is identical to the regular diffusion equation except for the additional "minus sign" in (1.13). Noting that it is possible to eliminate the minus sign in (1.13)–(1.15) by redefining time $t \rightarrow -t$ so that time will "run backwards," we now see the source of the nomenclature *the backwards diffusion equation* which is used in regard to the system (1.13)–(1.15).

Let us pause to consider the properties of the backwards diffusion equation. Suppose we set out as in the case of the classical diffusion equation to solve (1.13)–(1.15) using the method of separation of variables. This is readily seen to be formally possible, and it will yield that:

$$u(x, t) = \frac{A_0}{2} + \sum_{n=1}^{\infty} A_n e^{\frac{n^2 \pi^2}{L^2} t} \cos(n\pi x/L), \quad (1.19)$$

where the coefficients A_i , $i = 0, 1, 2, \dots$ are determined by the Fourier coefficients of the initial conditions,

$$u(x, 0) = u_0(x) = \frac{A_0}{2} + \sum_{n=1}^{\infty} A_n \cos(n\pi x/L), \quad (1.20)$$

i.e.,

$$A_i = \frac{2}{L} \int_0^L u_0(x) \cos(n\pi x/L) dx, \quad i = 1, 2, 3, \dots \quad (1.21)$$

These results are really not surprising. In fact the solution obtained above can also be obtained by simply setting $t \rightarrow -t$ in the separation of variables solution to the regular or "classical" diffusion equation.

Recall that in the case of the classical diffusion equation, the solution approaches a constant at large times. This can be seen by making the transformation $t \rightarrow -t$ in (1.20), (1.21) to obtain for the classical heat equation that

$$u(x, t) \rightarrow \frac{A_0}{2} \text{ as } t \rightarrow \infty.$$

On the other hand, we see from (1.20)-(1.21) that in the case of backwards diffusion, exponential growth will always be predicted unless $A_i = 0$, $i = 1, 2, \dots$. This is easy to make more precise. Defining

$$\|f\|_{L^2[0, L]}^2 := \langle f, f \rangle,$$

where

$$\langle f, g \rangle := \frac{2}{L} \int_0^L fg \, dx,$$

it follows from *Parseval's equality* (See Appendix A1.0.7.) that for the regular diffusion equation

$$\|u(x, t)\|_{L^2[0, L]}^2 = \frac{A_0^2}{2} + \sum_{n=1}^{\infty} A_n^2 e^{-\frac{2n^2\pi^2}{L^2}t}, \quad (1.22)$$

while for the backwards diffusion equation,

$$\|u(x, t)\|_{L^2[0, L]}^2 = \frac{A_0^2}{2} + \sum_{n=1}^{\infty} A_n^2 e^{\frac{2n^2\pi^2}{L^2}t}. \quad (1.23)$$

Moreover, from (1.22) and (1.23) it is readily verified that whereas the regular (or "forward") diffusion equation is well-posed, the backwards diffusion equation is *ill-posed*. Ill-posedness implies that arbitrarily small perturbations in the initial data can give rise to arbitrarily large changes in the solutions after a finite period of time (see Exercise 2), which certainly seems quite unnatural. While the ill-posedness of the backwards diffusion equation is clearly problematic, it has nevertheless been employed constructively in certain applications such as in image processing where the ill-posedness can be circumvented by seeking solutions within an appropriately bounded set [16]. For the Cahn-Hilliard equation, the ill-posedness of the backwards diffusion equation is avoided by the regularizing effects of the higher order terms, as we shall see in the sequel.

1.3 The Cahn-Hilliard equation and phase separation

Let us reflect for a moment on the solution to the backwards heat equation which we formally derived in the previous section, and let us recall that $u(x, t)$ is being taken to represent the concentration of one of the two components in a binary system. Hence, as noted earlier, $u(x, t)$ should satisfy $0 \leq u \leq 1$. We remark that indeed we do need to write here " \leq " and not simply " $<$ " since there is nothing unphysical about a system actually attaining the values 0 and 1; if $u(x, t) = 0$ or 1 at

some specific points in space-time in, say, an Fe-Al system, it simply means that the local composition of the material is either pure Fe or pure Al. Thus, for a solution to be physical, it should be bounded, and in fact it should be bounded between 0 and 1. However, the formal solution which we found to the backwards heat equation was ill-posed, and therefore cannot be guaranteed to maintain any bound even at short times. In particular, it cannot be expected to remain bounded between 0 and 1. Thus we see once more that the formal solution to the backwards heat equation which was obtained is unphysical. The implication here is that even if the full Cahn-Hilliard model is fairly physical, the simplifications made in Section 1.2 were too drastic to yield a reasonable physical description of phase separation.

Since the goal of this section is to demonstrate the connection between the Cahn-Hilliard equation and phase separation, we must see how by making less drastic simplifications and assumptions, a relatively credible physical picture of phase separation can be attained. To make progress in this direction, we now outline what are the physical features and phenomena which we should wish to describe with the Cahn-Hilliard equation.

As stated earlier, what we would like to describe is the dynamics of *pattern formation* which typify phase separation in two component systems. A typical scenario which we should like to be able to model is that of *quick quenching*, which may be described as follows. Let us consider some domain $\Omega \subset R^3$. For simplicity we may suppose that $\Omega = [0, L] \times [0, L] \times [0, L]$. And let us suppose that the domain Ω initially contains a two component system which is spatially uniform: $u(x, 0) = u_0(x) \equiv \bar{u}$, where, to be physical, the inequality $0 \leq \bar{u} \leq 1$ must hold. If we suppose that there is no flux of material into or out of the system under consideration, then the total amount of each component should be preserved over time. This implies that

$$\frac{1}{|\Omega|} \int_{\Omega} u(x, t) dx = \bar{u}, \quad 0 \leq t \leq T. \quad (1.24)$$

Let us suppose that initially the temperature is given by Θ_0 , and let us now cool the system (i.e., the cube of material contained in Ω), *very rapidly* to some lower temperature which we shall denote by Θ_1 . This is the process known as *quick quenching*. In certain systems, such as in certain polymer systems, quick quenching can actually refer to the *rapid heating* of the system from Θ_0 to some higher temperature Θ_1 . The working supposition here shall be that the temperature of the system

Fig. 1.1. A system quick quenched from (\bar{u}, Θ_0) to (\bar{u}, Θ_1^1) and from (\bar{u}, θ_0) to (\bar{u}, Θ_1^2) , where (\bar{u}, Θ_0) , (\bar{u}, Θ_1^1) , and (\bar{u}, Θ_1^2) are as indicated in the phase diagram in Figure 1.2.

equilibrates very rapidly to the new temperature, so that the temperature can be taken to be effectively equal to new temperature Θ_1 immediately throughout the system. In reality, the equilibration process cannot actually be immediate. However, if the thermal conductivity of the system is large, as it is for example in binary metallic alloys, then this does not constitute a bad approximation. Should we wish to take into account thermal variations in the system, we could couple the Cahn-Hilliard equation with an energy balance equation. This approach is indeed feasible, and the resultant system is known as a *conserved phase field model*. This system shall be discussed further in Section 13.1, but it is beyond the scope of this introductory discussion.

The dynamics which can be expected to appear in the system Ω in the wake of quick quenching can be explained roughly within the framework of classical thermodynamics with the help of *phase diagrams* using the approach of Gibbs [41]. This implies in particular that the expected behavior of the system can be determined by the values of certain *thermodynamic variables*. In the present context, the relevant thermodynamic variables would refer here to Θ_0 , Θ_1 , and \bar{u} , and whether or not phase separation would be predicted to occur, and the nature of the phase separation which would be expected to occur, would be determined by the location of (\bar{u}, Θ_0) and (\bar{u}, Θ_1) within the phase diagram. While phase diagrams of varying levels of complexity can occur, a simplest nontrivial

Fig. 1.2. A typical phase diagram in which (\bar{u}, Θ_0) lies above the binodal curve in the stable region, (\bar{u}, Θ_1^1) lies in the "metastable region" which lies between the spinodal curve and the binodal curve, and (\bar{u}, Θ_1^2) lies below the spinodal curve. See also Figure 1.1.

level of phase diagram which can describe phase separation is portrayed in Figure 1.2.

In terms of the phase diagram in Figure 1.2, there are two curves which should be noted. There is an upper curve, known as the *binodal* or the *coexistence curve*, and there is a lower curve, known as the *spinodal*. The two curves intersect at a point which is referred to as the *critical point* which we shall label as $(\bar{u}_{crit}, \Theta_{crit})$. In order for a system to be expected to undergo phase separation, its initial state (\bar{u}, Θ_0) should lie above both the binodal and spinodal, and its final state (\bar{u}, Θ_1) should lie somewhere below the binodal, either above or below the spinodal. The region above the binodal is known as the *stable* or *one-phase region*. If both (\bar{u}, Θ_0) and (\bar{u}, Θ_1) lie above the binodal, no phase separation is expected to occur and the system is expected to persist in its initially uniform state, $u(x, t) \equiv \bar{u}$.

If the system is cooled from above the binodal curve, to below the spinodal curve and $\bar{u} \neq \bar{u}_{crit}$, then phase separation is predicted to onset via a process known as *spinodal decomposition*. During this process the evolution of the system is distinguished by a certain "fogginess" reflecting the simultaneous appearance and growth of perturbations with many different wavelengths. Phase separation via spinodal decomposition is fairly well described within the framework of the Cahn-Hilliard

Fig. 1.3. Some effective time evolution snapshots of the system which has been quick quenched from (\bar{u}, Θ_0) to (\bar{u}, Θ_1^+) , which lies below the spinodal curve.

theory, and we will return to discuss it further shortly. See Figure 1.3 where some effective time evolution snapshots of a system which has been quick quenched below the spinodal curve. We refer to these snapshots as *effective* time evolution snapshots, since while it is very difficult experimentally to examine a specific specimen at different times, it is relatively feasible to view similar specimens at various times.

If the system is cooled from a state which lies above the binodal to a state which lies below the binodal but above the spinodal, then phase separation can be expected to onset via a process known as *nucleation and growth*. During this process, the uniform state $u(x, 0) \equiv \bar{u}$ gives way to a phase separated state, but no "fogginess" is seen. Instead, phase separation occurs via the appearance or *nucleation* of localized perturbations in the uniform state \bar{u} which persist and grow if they are sufficiently large. Smaller perturbations may also appear, but they afterwards in general shrink and disappear. The rate at which phase separation takes place via nucleation and growth increases with the distance of the final state below the binodal, and the size of the critical nuclei, that is the size that the localized perturbations must be in order to grow, decreases with distance below the binodal. Though we mention the process of nucleation and growth, we note that most of its features are less readily modelled within the Cahn-Hilliard framework. To describe nucleation and growth properly, alternative approaches such as the Lifshitz-Slyozov

Fig. 1.4. Some effective time evolution snapshots of the system quick quenched from (\bar{u}, Θ_0) to (\bar{u}, Θ_1^2) , which lies in the metastable region.

theory of *Oswald ripening* [63] and its extensions [51, 2] have been used to serve this purpose. See Figure 1.4.

We caution the reader that if $|\bar{u} - \bar{u}_{crit}| \ll 1$, $\Theta_0 > \Theta_{crit} > \Theta_1$, and $\Theta_{crit} - \Theta_1 \ll 1$, then the above descriptions are inappropriate. Phase separation will still take place but will be accompanied by certain *critical phenomena* [29], such as critical slowing down, which are characteristic of *second order* phase transitions. If $|\bar{u} - \bar{u}_{crit}| \ll 1$ and $\Theta_0 > \Theta_{crit} > \Theta_1$ and $\Theta_{crit} - \Theta_1 = \mathcal{O}(1)$, then our earlier descriptions, which are appropriate for *first order* phase transitions remain (essentially) correct. Arguably Θ_1 should be taken not too far from Θ_c , so that the phase separation will proceed sufficiently slowly, and hence that inertial and higher order effects can be neglected. Such effects would render the Cahn-Hilliard model inaccurate, and make it difficult to follow the phase separation and to control the resultant microstructure. What distinguishes a first order phase transition from a second or higher order phase transition is the degree of continuity or regularity of the system as the system crosses from the stable regime above the binodal into the *unstable* regime which lies below it. In a second order transition, the thermodynamic variables and their first derivatives are continuous, but not all of their second derivatives are. In a first order phase transition, the thermodynamic phase variables are continuous, but not all of their derivatives are. In the present context, the chemical potential is continuous across the the coexistence curve, but its derivative with respect

Fig. 1.5. Some effective time evolution snapshots of systems during the later stages of coarsening which commenced phase separation *i*) at (\bar{u}, Θ_1^1) and at *ii*) at (\bar{u}, Θ_1^2) .

to \bar{u} is not, unless the coexistence curve is crossed via the critical point $(\bar{u}_{crit}, \Theta_{crit})$ [64].

Whether the onset of phase separation occurs via spinodal decomposition or via nucleation and growth, eventually the system begins to saturate into spatial regions where $u \approx u_A$ or by $u \approx u_B$, where u_A and u_B denote the binodal or limiting miscibility gap concentrations when $\Theta = \Theta_1$. See (u_A, Θ_1) and (u_B, Θ_1) in Figure 1.2 and the experimental results in Fig. 1.5. The average size of these spatial regions increases over time, with the larger regions growing at the expense of the smaller regions. This process is called *coarsening*. After some period of time, most of Ω is dominated by the concentrations u_A and u_B , and the dominant feature of the dynamics is the motion of the boundaries or *interfaces* between the various regions where $u \approx u_A$ or $u \approx u_B$. Since the system is constrained to satisfy mass balance, (1.24) must be satisfied throughout the process of phase separation. This constitutes a constraint on the relative volume or area of the domains where $u \approx u_A$ and $u \approx u_B$. However, within the limitations of this constraint, the overall amount of interfaces continues to decrease as some limiting configuration is seemingly approached.

The question now arises as to what the Cahn-Hilliard equation can and cannot say with regard to this physical description. We have already hinted that nucleation and growth is somewhat of a weak spot

for the Cahn-Hilliard theory. However, before jumping into these details and more, it is convenient to sidestep the general formulation of the Cahn-Hilliard equation given in (1.1)-(1.3), and to consider some specific formulations. In this regard, we shall consider two particular formulations, though our later analysis will again be more general.

1.4 Two prototype formulations

Perhaps the easiest nontrivial formulation to consider is the formulation given in (1.4)-(1.6) which was introduced in the beginning of our discussion of the backwards diffusion equation. In this formulation the mobility was taken to be a positive constant and the homogenous free energy, as we shall see, corresponded to a quartic polynomial. For future reference, we shall refer to this case as *Case I*, which is summarized below.

Case I: The constant mobility - quartic polynomial case.

In *Case I*,

$$M(u) = M_0 > 0, \quad M_0 \text{ a constant, and } f(u) = -u + u^3. \quad (1.25)$$

Note that it follows from (1.25) that

$$f(u) = F'(u), \quad F(u) = \frac{1}{4}(u^2 - 1)^2. \quad (1.26)$$

Within the framework of (1.25), the Cahn-Hilliard equation is given by

$$u_t = M_0 \Delta(-u + u^3 - \epsilon^2 \Delta u), \quad (x, t) \in \Omega \times (0, T), \quad (1.27)$$

$$n \cdot \nabla u = n \cdot \nabla \Delta u = 0, \quad (x, t) \in \partial\Omega \times (0, T), \quad (1.28)$$

in conjunction with appropriate initial conditions. Clearly the value of M_0 may be changed by rescaling time. Hence if we wish we may set $M_0 = 1$. However, we maintain M_0 within the formulation (1.27)-(1.28), since typically it appears in the literature in this form [74]. Note that (1.27) is invariant under the transformation $u \rightarrow -u$. This it is natural to consider (1.27) for u in an interval which is symmetric about the origin, $u \in [-a, a]$. The formulation (1.27) is typically obtained by considering the dynamics for $u = c_A - c_B = 2c_A - 1$, where c_A satisfied a Cahn-Hilliard equation with constant mobility and a polynomial free energy; thus, $u(x, t)$ should assume values in the interval $[-1, 1]$.

Fig. 1.6. The initial stages of spinodal decomposition for *Case I*, based on the numerical scheme discussed in Chapter 12.

The analysis and treatment of *Case I* is relatively easy, at least initially. Existence, uniqueness, well-posedness, and regularity results are described in detail in Sections 5.1-5.2. Basically, (1.27)-(1.28) corresponds to a fourth order semilinear parabolic equation which is somewhat more complicated to treat than second semilinear parabolic equations, such as the reaction diffusion equation

$$u_t = \epsilon^2 \Delta u - f(u), \quad (1.29)$$

which arises in a wide variety of applications, from populations genetics to tiger spots, [70, 71]. Nevertheless, many of the tools which were developed for second order semilinear parabolic equations can be employed here also. However, the maximum principle, which is one of the mainstays in the treatment of second order equations, does not in general carry over into the fourth order setting [65]. An existence theory can be given in terms of Galerkin approximations [90, 96] which can also be used to construct finite element approximations that can be implemented numerically. From numerical calculations, it can be seen that for an appropriate choice of initial conditions, *Case I* gives a reasonable description of the spinodal decomposition process, see Figure 1.6. All these notions are amplified and explained in the Chapters which follow. See in particular Chapters 5, 6, 7, 8, and 12. An unfortunate feature of the Cahn-Hilliard variant which we have denoted by *Case I* is that its solutions need not always remain bounded between 0 and 1 even if the

initial data lies in this interval. This effect, which is clearly undesirable and unphysical, is demonstrated in Figure 1.7. In the formulation given below as *Case II*, this drawback is indeed avoided by making an appropriate choice of a free energy with logarithmic terms and of a *degenerate mobility*, in other words, a mobility which is not strictly positive [31]. We remark that an alternative approach is to work with say a polynomial free energy and with a degenerate mobility which vanishes at $u = -1$ and $u = 1$ (or at $u = 0$ and at $u = 1$), and to define solutions to be identically equal to -1 or 1 outside of the range $(-1, 1)$. This constitutes a *free boundary problem* approach to the Cahn-Hilliard equation, which under appropriate assumptions can be successfully implemented [80]. An example of such a formulation is given in Section 14.2.

Case II: The degenerate mobility - logarithmic free energy case.

In *Case II* we set

$$M(u) = u(1 - u), \quad \text{and} \quad f(u) = F'(u), \quad (1.30)$$

where

$$F(u) = \frac{\Theta}{2} \{u \ln u + (1 - u) \ln(1 - u)\} + \alpha u(1 - u), \quad (1.31)$$

with $\Theta > 0$, $\alpha > 0$, where Θ denotes temperature, or more accurately a scaled temperature. Here the resultant Cahn-Hilliard formulation is given by:

$$\begin{aligned} u_t &= \nabla \cdot M(u) \nabla \left\{ \frac{\Theta}{2} \ln \left[\frac{u}{1-u} \right] + \alpha(1 - 2u) - \epsilon^2 \Delta u \right\}, & (x, t) \in \Omega_T, \\ n \cdot \nabla u &= 0, & (x, t) \in \partial\Omega_T, \\ n \cdot M(u) \left\{ \frac{\Theta}{2u(1-u)} \nabla u - 2\alpha \nabla u - \epsilon^2 \nabla \Delta u \right\} &= 0, & (x, t) \in \partial\Omega_T, \end{aligned}$$

where $\Omega_T = \Omega \times (0, T)$, $\partial\Omega_T = \partial\Omega \times (0, T)$. Formally, since $M(u) = u(1 - u)$, it can be written more simply as

$$u_t = \frac{\Theta}{2} \Delta u - \nabla \cdot M(u) \nabla \{2\alpha u + \epsilon^2 \Delta u\}, \quad (x, t) \in \Omega_T, \quad (1.32)$$

$$n \cdot \nabla u = n \cdot M(u) \nabla \Delta u = 0, \quad (x, t) \in \partial\Omega_T. \quad (1.33)$$

Again the equation and boundary conditions must be considered in conjunction with appropriate initial conditions. Within the context of this formulation, $u(x, t)$ is taken to represent concentration of one of the two components, and hence should satisfy $0 \leq u(x, t) \leq 1$.

The mobility in (1.30) is referred to as a *degenerate* mobility, since it is not strictly positive and can vanish over the domain of interest, $0 \leq u \leq 1$. It is interesting to note that a concentration dependent mobility was already considered by Cahn in 1961 [13]. In fact a *degenerate mobility* similar to (1.30) had already been included by Hillert in his 1956 formulation [49, 48] of a one-dimensional discretely defined precursor of the Cahn-Hilliard equation. The use of a logarithmic free energy, which arises naturally from thermodynamic considerations as we shall explain in Chapter 2, also actually appeared already in the work of Hillert [49, 48] as well as in the 1958 paper of Cahn and Hilliard [14] in their discussion of the free energy. However, very rapidly the degenerate and concentration dependent mobilities were replaced by constant mobilities and the logarithmic terms were expanded into polynomials, in order to simplify the problem and to allow at least some progress to be made in regard to the qualitative behavior of the equation. In fact, early analyses were totally linear, as the inclusion of nonlinear terms in the free energy in a higher order equation was found to be much of a challenge. The first one to include even these nonlinear terms was deFontaine [27], who did so in the context of his early numerical studies of the Cahn-Hilliard equation.

The problem which we have formulated as *Case II* can be described as a degenerate fourth order semilinear parabolic problem. Galerkin approximations can be used to prove existence, which in turn can be used to construct finite element approximations that can be implemented numerically. However the degeneracy of the mobility and the singularity in the logarithmic terms give rise to various technical complications. Basically a way to overcome these difficulties is to approximate $M(u)$ using *nondegenerate* (nonvanishing) mobilities and to approximate $f(u)$ using *nonsingular* approximants. The details with regard to existence for *Case II* are given in Chapter 11, and the details with regard to numerical schemes for *Case II* are given Chapter 12. One of the rewards for working with this more complicated formulation lies in the fact that within the context of this model, if $0 \leq u_0(x) \leq 1$, then $0 \leq u(x, t) \leq 1$ for $t \geq 0$, as shall be demonstrated in detail in Chapter 11.

Chapter 2, which follows, contains a derivation of both of the above Cahn-Hilliard variants. It is more natural to first justify the physically more realistic formulation of the Cahn-Hilliard equation given above as *Case II* and then to obtain *Case I* by making appropriate simplifying assumptions; this is the approach which is adopted in the derivation given in Chapter 2.

Fig. 1.7. A numerical run of the *Case I* variant of the Cahn-Hilliard equation from which it can be seen that solutions which begin within the interval $[0, 1]$, need not stay there. For the numerical method, see Chapter 12.

In terms of spinodal decomposition, it turns out that during the early stages of phase separation nonlinear effects are not of primary importance and linear stability analysis can provide considerable insight into the process. Moreover, when $0 \leq u_0 \leq 1$, $0 < \bar{u}_0 < 1$, and $f'(\bar{u}_0) < 0$ the results for *Cases I* and *II* are not too different. While this may not be immediately obvious, it can be roughly explained as follows. The constraint $f'(\bar{u}_0) < 0$ can be seen to imply that \bar{u}_0 is bounded away from the values $\{0, 1\}$ which are problematic for *Case II*. Well-posedness then implies that $u(x, t)$ remains bounded away from the problematic values $\{0, 1\}$ over some finite period of time. During this initial interval, spinodal decomposition can start to get underway. Hence, perhaps it is not surprising that the initial behaviors are not too unsimilar. See Figures 1.6 and 1.8. Further details concerning the initial behavior are given in Chapter 6.

As time goes on, the importance of the nonlinear terms becomes more and more pronounced. It is the nonlinear effects which keep the amplitude of the solution from becoming unbounded and which cause the system to saturate near the binodal values, u_A and u_B . After the initial stages of saturation, certain regions, in which u_A or u_B dominate, grow at the expense of other regions. Within the context of the Cahn-Hilliard theory it is possible to obtain predictions for the motion of the partitions between the u_A regions and the u_B regions. These partitions are

Fig. 1.8. The initial stages of spinodal decomposition for *Case II*, based on the numerical scheme discussed in Chapter 12.

commonly referred to as *interfaces* and the concentrations u_A and u_B are referred to as the *phases*. This process is known as *coarsening*. The differences between the two Cahn-Hilliard variants becomes more pronounced during coarsening than during spinodal decomposition. This is due in part to the proximity of the binodal concentrations u_A and u_B to the points of degeneracy of the mobility in the *Case II*. Some of these differences will be further amplified in Section 1.5.

An obvious question which arises is experimental verification of the Cahn-Hilliard theory. While it can be seen from the figures which have been presented in this chapter that the qualitative comparison between experimental and numerical data seems reasonable, a more quantitative test is clearly desirable. An approach which has been developed to study and compare the evolution of various physical systems undergoing phase separation with the predictions of numerical solutions to the Cahn-Hilliard equation is by using the *structure function* which can be defined as:

$$S(k, t) = |\{u - \bar{u}\}^\wedge(k, t)|^2$$

where $\bar{u} = \bar{u}(t) := \frac{1}{|\Omega|} \int_{\Omega} u(x, t) dx$, and " \wedge " denotes the Fourier transform. When the characteristic length scale of the features of the system are much smaller than the characteristic size of the system, it is reasonable to ignore edge effects and to take $\Omega \approx R^n$. Under these

Fig. 1.9. Comparison of experimental and numerical results for the structure function $S(k, t)$, within the context of *Case I*.

circumstance, if the system in question is effectively two dimensional, then

$$S(k, t) \approx \frac{1}{4\pi^2} \left| \int_{R^2 \times R^2} f(\bar{x}, t) f(\bar{y}, t) e^{-k \cdot (\bar{x} - \bar{y})} d\bar{x} d\bar{y} \right|^2, \quad \forall k \in R^2, \quad (1.34)$$

where $f(s, t) = u(s, t) - \bar{u}(t)$. The structure function can be used as a basis of comparison from the earliest stages and throughout the coarsening regime. For example as coarsening occurs, the average size of the regions where $u \approx u_A$ or $u \approx u_B$ grows, so that the dominant wavenumbers, k , which have the dimensions of length^{-1} , can be expected to become smaller. This behavior can be seen in Figures 1.9 and 1.10 where $S(k, t)$ is portrayed for experimental data as well as for the numerical calculations portrayed in Figures 1.6 and 1.8, for *Cases I* and *II* respectively. Various conjectures and studies have been made for the time evolution of the structure function and for possible self-similar behaviors, see *e.g.* [36]. Although the majority of these conjectures have yet to be rigorously verified, some rigorous results giving upper bounds on coarsening rates have been given [59].

Recently some more refined computational tools based on Betti numbers have been developed to study the topological changes which occur during phase separation [39]. Betti numbers, β_k , $k = 0, 1, \dots$, are topological invariants which is to say that they are numbers (indices) assigned to a spatial structure which remain unchanged under continuous

Fig. 1.10. Comparison of experimental and numerical results for the structure function $S(k, t)$, within the context of *Case II*.

deformation and which reflect the topological properties of the structure [55]. The first Betti number, β_0 gives a count of the number of connected components, and the second Betti number, β_1 gives a count of the number of loops (in two dimensions) or the number of tunnels (in three dimensions). Reasonable qualitative agreement between theory and experiment [52] has been reported in these studies.

1.5 Long time behavior and limiting motions

We should like to be able to describe coarsening, and in particular we should like to be able to get a hold on a description of the motion of the interfaces. It is within this context that the Mullins-Sekerka problem and motion by surface diffusion appear. These both constitute *free boundary problems* where by free boundaries we are referring in this context to the interfaces between the phases. We remarked earlier that *Cases I* and *II* differ in their behavior during the later coarsening stages, and indeed this can be seen in the fact that the behavior for *Case I* of the Cahn-Hilliard equations at long times can be described by the *Mullins-Sekerka* problem, and the behavior for *Case II* of the Cahn-Hilliard equation is described by *surface diffusion* if $\Theta = \mathcal{O}(\epsilon^{1/2})$. We note that the Mullins-Sekerka problem and motion by surface diffusion should not be viewed only as consequences of the Cahn-Hilliard equation; both first appeared earlier in various other problems in materials science [69, 4].

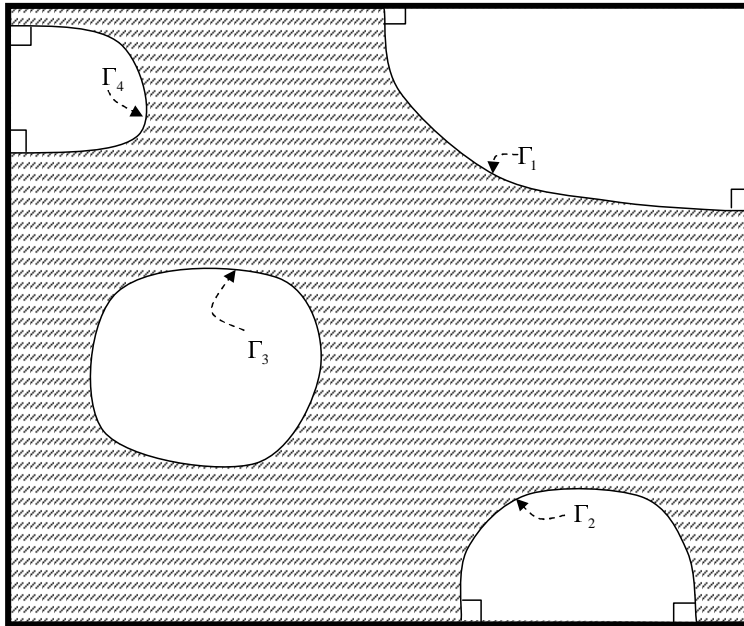


Fig. 1.11. A schematic portrayal of a system during coarsening

How now do we pass from the Cahn-Hilliard equation which describes the evolution of the concentration at all points in the system, to a description which focuses on the evolution of the interfaces during the coarsening period? One possibility is to derive the limiting motions mentioned above from the Cahn-Hilliard equation by utilizing certain formal asymptotic expansions [86, 12]. We shall see in the Chapter 8 and in Section 11.3 how this can be undertaken, and the necessary asymptotic tools will be defined and developed there. A more difficult task is to rigorously justify the formal asymptotic analysis. Under appropriate assumptions, the passage from the Cahn-Hilliard equation to the Mullins-Sekerka problem can be made rigorous [1, 20]. However, so far, the passage to motion by surface diffusion from the degenerate Cahn-Hilliard equation has yet to be rigorously justified, although numerical computations indicate that the limiting motion has been correctly identified [6].

Since coarsening is supposed to describe the evolution of the limiting motion after the system has sufficiently saturated near the binodal concentrations, we shall assume that during coarsening the domain Ω can

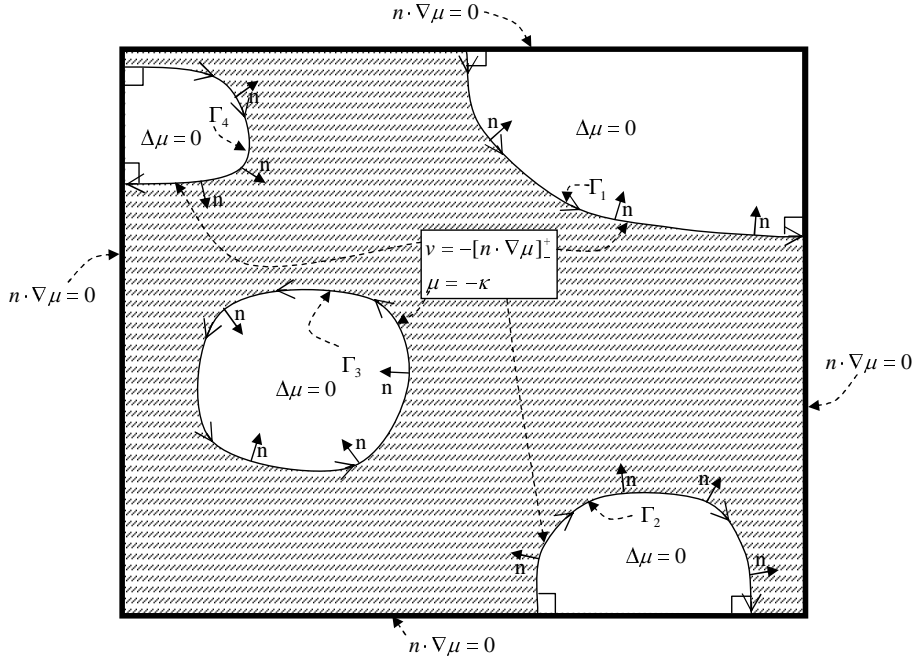


Fig. 1.12. Limiting motion as $t \rightarrow \infty$ for Case I: the Mullins-Sekerka problem.

be envisioned as being partitioned by N interfaces, Γ_i , $i = 1, \dots, N$, and that the description of the evolution of the system can be given in terms of these N partitions, see Figure 1.11.

The Mullins-Sekerka Problem

For *Case I*, the following laws are seen to govern the evolution of the system of interfaces, $\Gamma = \Gamma_1 \cup \Gamma_2 \cup \dots \cup \Gamma_N$. For $t \in (0, T)$, $0 < T < \infty$, away from the interfaces

$$\Delta\mu = 0, \quad x \in \Omega \setminus \Gamma, \quad (1.35)$$

and along the interfaces

$$V = -[n \cdot \nabla\mu]_{\pm}^{\pm}, \quad x \in \Gamma, \quad (1.36)$$

and

$$\mu = -\kappa. \quad (1.37)$$

In (1.35)-(1.37), $\mu = \mu(x, t)$ denotes the chemical potential which will be discussed further in the next chapter. In terms of the original

formulation $\mu = f(u) - \epsilon^2 \Delta u$. Note that in the limiting problem, the concentration $u = u(x, t)$ no longer appears explicitly, but only via the chemical potential, μ . In (1.36), $V = V(x, t)$ denotes the normal velocity at a given point $x \in \Gamma$, and $n = n(x, t)$ denotes a unit exterior normal to one of the components Γ_i which comprises Γ , assuming that orientations have been arbitrarily chosen for the parameterizations of the curves Γ_i , $i = 1, \dots, N$. Here the normal velocity V is prescribed by $V = n \cdot \vec{V}$ where $\vec{V} = \vec{V}(x, t)$ denotes the velocity at $x \in \Gamma$. See Gurtin [45] for background. Note that Γ is also actually time dependent in this formulation. The expression $[n \cdot \nabla \mu]_+^+$ denotes the jump in the normal derivative of μ across the interface at $x \in \Gamma$. In (1.37), κ denotes the mean curvature. For curves in the plane, the mean curvature $\kappa = \kappa(x)$ is given by

$$\kappa = \frac{1}{R},$$

where R is the *signed radius* of the inscribed circle which is tangent to Γ at $x \in \Gamma$. The sign of the radius is taken here to be positive if the inscribed circle lies on the "exterior" or "left" side of the curve whose orientation has been fixed. For interfaces (hypersurfaces) in R^3 , κ is given by

$$\kappa = \frac{1}{2} \left(\frac{1}{R_1} + \frac{1}{R_2} \right),$$

where R_1 and R_2 denote the *principle radii of curvature*. See Gurtin [45] for a discussion in R^2 , and Finn [33] or do Carmo [28] for precise definitions in R^3 .

Along the boundary of the domain Ω ,

$$\mathbf{n} \cdot \nabla \mu = 0, \quad x \in \Gamma \cap \partial\Omega, \quad (1.38)$$

and

$$\Gamma \perp \partial\Omega, \quad x \in \Gamma \cap \partial\Omega. \quad (1.39)$$

The system of equations and conditions given above in (1.35)-(1.39) together constitute the Mullins-Sekerka problem [69]. Clearly it is a *nonlocal problem* in that we can not ascertain the motion of the interfaces without taking into consideration what is happening within the regions bounded by the interfaces. In Chapter 8 a formal asymptotic derivation of these laws governing the limiting motion will be presented, some properties of the Mullins-Sekerka system will be given, and the method by which the system can be justified as a limiting motion will also be outlined.

Surface Diffusion

In Case II, if $\Theta = \mathcal{O}(\epsilon^{1/2})$, then at long times after a suitable amount of preliminary saturation has occurred, the limiting motion in the degenerate-logarithmic case is given by

$$V = -\frac{\pi^2}{16}\Delta_s\kappa, \quad x \in \Gamma. \quad (1.40)$$

Here V , κ and Γ have the same connotations as in the discussion of the Mullins-Sekerka problem given above, and Δ_s denotes the *surface Laplacian*, known also as the *Laplace-Beltrami operator*. Along curves in the plane one has that

$$\Delta_s\kappa = \kappa_{,ss},$$

where s refers to an arc-length parameterization of the components of Γ ; i.e., along Γ_i , $i \in \{1, \dots, N\}$,

$$s(p) = \int_{p_0}^p \sqrt{\dot{x}^2 + \dot{y}^2} d\tau,$$

where $\{x(\tau), y(\tau) \mid p_0 \leq \tau \leq p\}$ denotes an arbitrary parameterization of Γ_i and p_0 refers to an arbitrary point on Γ_i . For a more general definition of the surface Laplacian, see [38] or the discussion in Section 11.3 where (1.40) is derived. Equation (1.40) is to be solved in conjunction with a no-flux boundary condition where interfaces intersect the exterior boundary of the domain $\partial\Omega$ which may be written as

$$\mathbf{n} \cdot \nabla_s \kappa = 0, \quad x \in \Gamma \cap \partial\Omega \quad (1.41)$$

and the curves Γ_i which comprise Γ should intersect the exterior boundary normally,

$$\Gamma_i \perp \partial\Omega, \quad i = 1, \dots, N, \quad x \in \Gamma \cap \partial\Omega. \quad (1.42)$$

In the plane the boundary condition (1.41) may be written simply as

$$\kappa_s = 0, \quad x \in \Gamma \cap \partial\Omega.$$

at intersections of Γ with $\partial\Omega$.

The motion here is *geometric* in that it is not necessary to know what is happening away from the interfaces $\{\Gamma_i\}_{i=1}^N$ in order to ascertain the resultant motion. A formal asymptotic derivation of (1.40)-(1.42) is presented in Chapter 11. We remark that the system (1.40)-(1.42) can also be shown to describe the long time limiting motion for the *deep quench limit* [12]; the deep quench limit is an obstacle problem which is obtained from *Case II* in the limit $\Theta \downarrow 0$. See Chapter 10 for details.

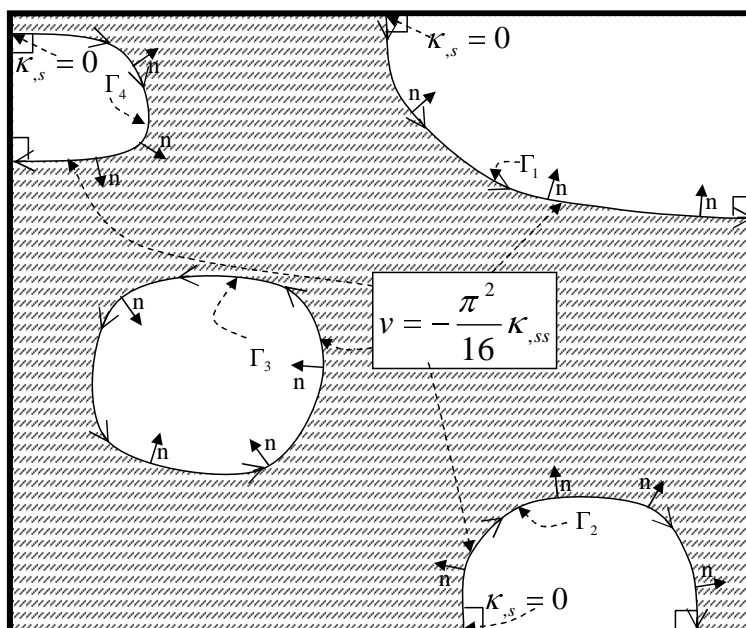


Fig. 1.13. Limiting motion as $t \rightarrow \infty$ for *Case II*: Motion by surface diffusion.

Exercises

- 1.1 Verify the solution (1.19)–(1.21) given above.
- 1.2 Prove that the backwards diffusion equation is *ill-posed*; i.e., for any $\delta > 0$, $C > 0$, and $\bar{t} > 0$, there exists an initial perturbation $\tilde{u}_0 \in L^2[0, L]$ such that $\|\tilde{u}_0\|_{L^2[0, L]} < \delta$ and the solution, $\tilde{u}(x, t)$, to (1.13)–(1.15) satisfies $\|\tilde{u}(x, \bar{t})\|_{L^2[0, L]} > C$. Hint: It suffices to consider perturbations of the form $\tilde{u}_0 = A_k \cos(k\pi x/L)$.
- 1.3 Suppose that Ω is a circular domain in the plane with radius R_1 whose center lies at the origin in R^2 , and that Ω contains only one interface which we shall denote as Γ_1 , $\Gamma_1 = \Gamma_1(x, t)$. Suppose that at time $t = 0$, Γ_1 constitutes a circle with radius R_0 , $0 < R_0 < R_1$, whose center lies at the origin. Under the assumption that the motion of $\Gamma_1 = \Gamma_1(x, t)$ is governed by the Mullins-Sekerka problem, find the shape of Γ_1 at times $0 < t < \infty$.
- 1.4 Suppose as in Exercise 3 that Ω is a circular domain in the plane whose radius is $R_1 > 0$ and whose center lies at the origin in

R^2 , and that Ω contains one interface, Γ_1 , $\Gamma_1 = \Gamma_1(x, t)$. Under the assumption that at time $t = 0$, Γ_1 constitutes a circle with radius R_0 , $0 < R_0 < R_1$, whose center lies at the origin, find the location of Γ_1 at times $0 < t < \infty$ if the motion of Γ_1 is governed by surface diffusion.